Intermediate Filaments Regulate Tissue Size and Stiffness in the Murine Lens

Douglas S. Fudge,[1] John V. McCuaig,[1] Shannon Van Stralen,[1] John F. Hess,[2] Huan Wang,[3] Richard T. Mathias,[3] and Paul G. FitzGerald[2]

Purpose. To define the contributions of the beaded filament (BF), a lens-specific intermediate filament (IF), to lens morphology and biomechanics.

Methods. Wild-type and congenic CP49 knockout (KO) mice were compared by using electrophysiological, biomechanical, and morphometric approaches, to determine changes that occurred because of the absence of this cytoskeletal structure.

Results. Electrophysiological assessment established that the fiber cells lacking the lens-specific IFs were indistinguishable from wild-type fiber cells. The CP49 KO mice exhibited lower stiffness, and an unexpected higher resilience than the wild-type lenses. The absence of these filaments resulted in lenses that were smaller, and exhibited a higher ratio of lens:lens nucleus size. Finally, lens shape differed as well, with the CP49 KO showing a higher ratio of axial:equatorial diameter.

Conclusions. Previous work has shown that BFs are necessary in maintaining fiber cell and lens structural phenotypes with age, and that absence of these filaments results in a loss of lens clarity. This work demonstrates that several tissue-level properties that are critical to lens function are also dependent, at least in part, on the presence of these lens-specific IFs. (*Invest Ophthalmol Vis Sci.* 2011;52:3860–3867) DOI:10.1167/iovs.10-6231

One of the greatest challenges of the postgenomic era in biology is to understand the relationships among gene expression, cell phenotype, and tissue architecture and their function within whole organisms. The ocular lens is one of the best examples of a tissue in which precise tissue morphology and finely tuned mechanical properties are critical to function. The lens must not only be optically clear, but must also assume and maintain a shape that focuses light on a narrow (~60 μm) layer of the retina.[1] Furthermore, in accommodating animals, the lens must be able to change shape to mediate a shift in focal point between near and far objects and then recover its exact starting shape. The mammalian lens is flattened when zonular fibers exert tension around its equator. When circular ciliary muscles contract, they release the tension on zonular fibers, and the lens recovers its more rounded shape by passive elastic recoil.[2] The mechanical properties of the lens must therefore be permissive to shape change, but also exhibit the ability to elastically recover its starting shape within very narrow tolerances.

The lens has many unusual properties that enable it to adapt to its unique function. To minimize light absorbance and scatter, the lens lacks blood vessels, nerves, and connective tissue and consists of a single cell type that ranges from the relatively undifferentiated lens epithelium, to the highly differentiated lens fiber cells. The latter constitute most of the lens volume.[3–5] One of the most striking features of vertebrate lenses is the tissue-level organization of fiber cells. These highly elongated cells (~2 × 5 × 10,000 μm in humans) are aligned and stacked with an unparalleled degree of order and precision,[6–8] a tissue-level attribute that has been demonstrated to be critical for optical clarity.[9,10] To further reduce light scatter, the process of differentiation from epithelial cell to fiber cell results in the elimination of all membranous organelles in the mature fiber cell. In the human lens, for example, only the outer 15% of the lens radius contains fiber cells that still possess organelles.[3,11–13] This differentiation process is rapid earlier in life, and although it slows, it does not cease. Because older fiber cells do not disappear, each new generation of fiber cells adds to the diameter of the lens, resulting in a continued growth in lens volume throughout life. This growth pattern results in an exact chronological arrangement of fiber cells, ranging from those that differentiated in the embryonic period (at the center of the lens), to the most recently differentiated (at the surface). Over time, the fiber cells in the central lens become more compacted, resulting in a stiffer, central region called the lens nucleus.[14]

Differentiation of the fiber cells includes the expression of two lens-specific members of the intermediate filament (IF) family: CP49 and filensin.[15–17] These proteins co-assemble into structurally distinct IFs, referred to as beaded filaments (BFs),[18,19] which represent the dominant cytoskeletal element of the mature fiber cell.[20,21] In previous work we have shown that both proteins are required for assembly of the BF and that knockout of either one results in the absence of the filaments, as well as almost complete knockdown of the assembly partner.[20,21] Surprisingly, the dramatic structural changes that accompany the differentiation of lens fiber cells from lens epithelial cells and the appearance of long-range stacking and order proceed normally in the CP49 KO lenses. However, with age, both the cells and the tissue are unable to maintain their highly ordered phenotypes, resulting in a randomization of structure that causes a progressive increase in light scatter and degradation of the optical properties of the lens.[9,10] Thus, CP49 KO mice are born with optically clear lenses, but undergo a progressive degradation in optical quality with age.

From the [1]Department. of Integrative Biology, University of Guelph, Guelph, Ontario, Canada; the [2]Department of Cell Biology and Human Anatomy, School of Medicine, University of California, Davis (UCD), Davis, California; and the [3]Department of Physiology and Biophysics, State University of New York, Stony Brook, New York.

Supported by National Institutes of Health Grant R01 EY08747 (PGF) and National Eye Institute Grants P30 EY12576 (UCD) and EY06391. The work was conducted in a facility constructed with support from Research Facilities Improvement Program Grant Number C06 RR-12088-01 (UCD) from the National Center for Research Resources, National Institutes of Health.

Submitted for publication July 15, 2010; revised November 19, 2010; accepted December 19, 2010.

Disclosure: **D.S. Fudge**, None; **J.V. McCuaig**, None; **S. Van Stralen**, None; **J.F. Hess**, None; **H. Wang**, None; **R.T. Mathias**, None; **P.G. FitzGerald**, None

Corresponding author: Paul G. FitzGerald, Department of Cell Biology and Human Anatomy, School of Medicine, University of California, Davis, CA 95616; pgfitzgerald@ucdavis.edu.

This progression is similar to that seen in humans with mutations in CP49, in that these individuals are born with clear lenses, but by young adulthood develop opacities that require lens replacement.[22,23] Thus, although not required to achieve the differentiated cellular and tissue level phenotypes, these lens-specific IFs are necessary in maintaining those phenotypes with age.

IFs in other tissues, such as cytokeratins in the epidermis[24,25] and desmin in muscle,[26,27] have been shown to play important roles in maintaining cell and tissue integrity. IFs have also been shown to contribute directly to cell stiffness in cultured cells,[28] and computational models suggest that IFs are most important for cell mechanics when there is extensive cell strain.[29] It therefore seemed reasonable to hypothesize that these lens-specific IFs contribute to the mechanical properties of both lens cells and lens tissue, which are essential for normal lens function. Specifically, we predicted that BFs function in tuning the stiffness of the lens. Stiffness is the relationship between load and deformation, and we expected lenses with fiber cells possessing intact BF networks to deform less for a given load than lenses lacking BF reinforcement.

In animals that accommodate, the lens must also be a highly elastic material. It is deformed by tension exerted by the zonular fibers on the lens equator during focusing on distant objects, but can only return to a more spherical shape for focusing on near objects via elastic recoil. We therefore expected that lens-specific IFs could be involved in imparting to the lenses the resilience they need to deform and recover elastically countless times over the lifetime of the animal. This idea is also consistent with recent data that suggest that IFs in cells act like a network of rubber bands up to modest cell strains.[30,31]

In this study, we measured the mechanical response of lenses from wild-type (WT) and BF knockout (CP49 KO) mice to test the hypothesis that BFs are an important determinant of lens stiffness and resilience. The fact that the lens lacks connective tissue, blood vessels, and nerves and is dominated by a single cell type, which in turn is dominated by a single IF type, affords a unique opportunity to isolate the contributions of an IF to overall tissue function. We show here that the absence of the lens-specific IF cytoskeleton leads to decreased stiffness and a surprisingly greater ability to elastically recover from compressional strains. We also show that the absence of BF results in significant changes in lens morphometrics, with CP49 KO mice possessing lenses that are smaller and differently shaped than their WT counterparts.

METHODS

Experimental Animals

CP49 KO mice were generated as described elsewhere.[21] These animals lacked both the CP49 protein and BF. The knockout animals used in this study had been created in the 129SvJ strain, but were backcrossed to C57BL/6J for 12 generations to achieve congenicity. C57BL/6J mice were used as controls. We specifically verified that the CP49 locus was the WT and did not contain the mutation that is common to many strains of mice.[32,33] Preliminary mechanical tests and previous work suggested that lens size and age could be significant determinants of lens material properties. We therefore measured the mechanical responses of lenses obtained from three age groups: young (~5 weeks, 30–39 days; n = 16 WT, n = 8 CP49 KO), middle-aged (~12 weeks, 82–88 days; n = 14 WT, n = 6 CP49 KO), and old (~24 weeks, 162–188 days, n = 7 WT, n = 7 CP49 KO). Mice were euthanized with CO_2 overdose in accordance with the Canadian Council on Animal Care (University of Guelph Animal Utilization Protocol 07R067) and the ARVO Statement for the Use of Animals in Ophthalmic and Vision Research.

Impedance Measurements

To ensure that the fiber cells of the CP49 KO lenses were viable, we made impedance measurements in both WT and CP49 KO lenses, as described previously.[34] Briefly, WT and CP49 KO mice were killed by intraperitoneal injection of sodium pentobarbital solution (100 mg/kg of weight). The eyes were removed and the lenses dissected from them and mounted on a silicone (Sylgard; Dow Corning, Midland, MI) base.

One microelectrode (current electrode) was used to inject a random current of selected bandwidth into a central fiber cell. A second microelectrode (voltage electrode) recorded the induced voltage at different depths. Impedance was calculated in real time by a fast Fourier analyzer (model 5420A; Hewlett-Packard Co., Palo Alto, CA). The impedance data were curve fit with a model of the lens to determine membrane resistances. The series resistance (R_S), defined in equations 1 and 2, was used to evaluate gap junction coupling.

$$R_S = \frac{1}{4\pi}\int_r^a \frac{R_i}{\rho^2}\,d\rho \qquad (1)$$

At sinusoidal frequencies approaching 1 kHz, the induced intracellular and extracellular voltages become nearly identical and are given by IR_S, where I is the injected current and R_S (in ohms) is the cumulative series resistance between the point of voltage recording (r) and the lens surface (a, both centimeters from the center). The effective intracellular resistivity, R_i (ohms-centimeter), is due mainly to the gap-junctional–coupling resistance between the point of recording and the lens surface. We have determined that R_i changes at the transition between differentiated (DF) and mature (MF) fiber cells (defined as $r = b$). Integrating equation a gives:

$$R_S = \frac{R_{DF}}{4\pi}\left(\frac{1}{r}-\frac{1}{a}\right)$$

$$R_S = \frac{R_{DF}}{4\pi}\left(\frac{1}{b}-\frac{1}{a}\right) + \frac{R_{MF}}{4\pi}\left(\frac{1}{r}-\frac{1}{b}\right) \qquad b \le r \le a \qquad (2)$$

where R_{DF} is R_i in DF and R_{MF} is R_i in MF. The coupling conductance per area of cell-to-cell contact $G_{DF,MF}$ (S/cm^2) is given by $1/(wR_{DF,MF})$, where $w \approx 3$ μm is the fiber cell width.

Morphometrics

After dissection from the eye, the lenses were quickly transferred to DMEM tissue culture medium, carried to the balance and blotted dry before weighing. Lens weight was measured to the nearest 0.1 mg on a balance (model SI-234; Denver Instrument, Bohemia, NY), and the lens was reimmersed in medium for transport to the mechanical testing chamber. Axial and equatorial diameters were measured (in pixels) from stills taken from an HD video recorded before the beginning of lens mechanical testing (Fig. 1). Diameter measurements in pixels were converted to millimeters with a calibration conversion obtained from an image of a ruler held at the exact position of the lens during testing. Additional calibration information was provided by a pretest movement of the compressor exactly 1 mm away from the lens. Lens volume was calculated from axial and equatorial diameter measurements by assuming that the lens is an ellipsoid and using the following equation:

$$V = \tfrac{4}{3}\pi r_{eq}^2 r_{ax} \qquad (3)$$

Nuclear diameter measurements were taken from video stills before the beginning of mechanical testing, if possible. In lenses in which the nucleus was not visible, the boundary between the cortex and the nucleus was sometimes revealed after mechanical testing was complete by subjecting the lenses to a large compression (0.66 mm), which often caused a visible shear plane between the cortex and nucleus. In

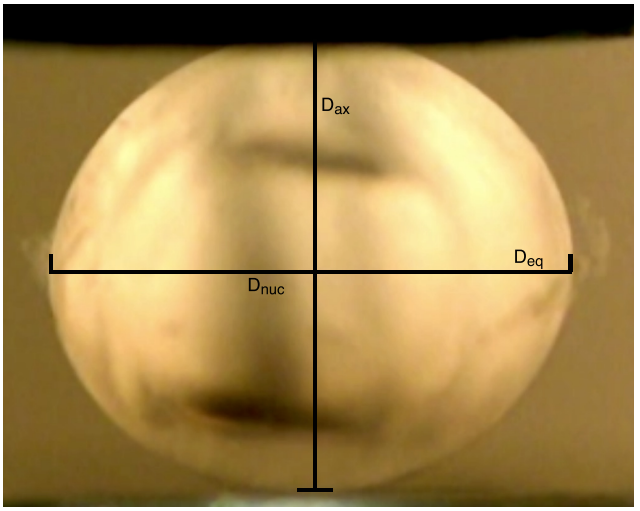

FIGURE 1. Video capture from a lens-compression trial showing axial and equatorial diameter measurements (D_{ax} and D_{eq}).

lenses from young mice of both genotypes, the nucleus was typically not visible, even after this treatment.

Mechanical Characterization

Lens mechanics were characterized within a custom glass testing chamber with flat sides that allowed us to capture the entire procedure with a video camera (Vixia HV30 HD; Canon; Tokyo, Japan) fitted with a macro conversion lens (model MSN-505; Raynox, London, UK). The glass testing chamber mounted on the base of a bench top universal testing system (model 3343; Instron, Norwood, MA) run by allied software (Bluehill ver. 9; Instron) and fitted with a 10-N load cell with a force resolution of 0.5 mN. Lenses were transferred from the medium and placed anterior side down on an aluminum pedestal within the empty chamber and held in place by bringing down the aluminum compression element until it just contacted the lens and held it in place. The chamber was then filled with 25 mL of 37°C DMEM medium before the commencement of mechanical testing.

Mechanical testing was performed with the custom compressional straining method described in Figure 2. Force and displacement data were collected every 0.1 second during the testing protocol. Raw force data were converted to compressional force by subtracting the net buoyant force exerted on the load cell as the aluminum compression

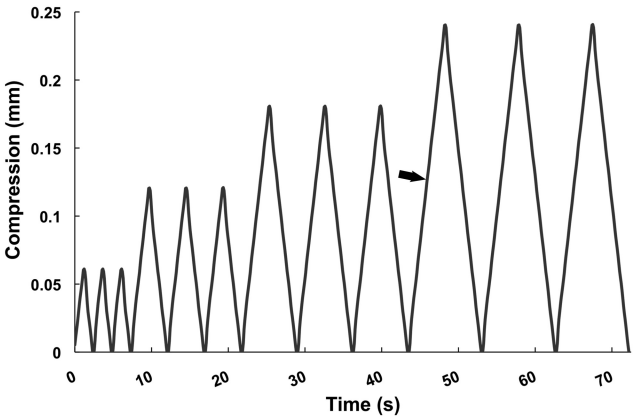

FIGURE 2. Strain regimen used to measure mouse lens mechanical properties. Stiffnesses were calculated from data collected during the loading portion (*arrow*) of the first 0.24-mm compression cycle, and resilience data were calculated from the loading and unloading data from this cycle.

TABLE 1. Results from Whole Lens Impedance Studies

	WT	CP49 KO
Lens radius, cm	0.120 ± 0.001	0.117 ± 0.001
Input resistance, kΩ	3.4 ± 0.3	3.5 ± 0.4
Resting voltage, mV	−62 ± 4	−61 ± 2
G_{DF}, S/cm^2	0.50	0.50
G_{MF}, S/cm^2	0.33	0.32

G_{DF} is the coupling conductance per area of cell-to-cell contact in the differentiated fiber cells and G_{MF} is the coupling conductance for mature fiber cells. There were no significant differences between four month old WT (n = 10) and CP49 KO (n = 6) mice in any of the transport parameters measured.

element was immersed in the medium. Lens stiffness (in millinewtons per millimeter) was calculated from the slope of the loading portion of the force displacement curve from the final 0.24-mm compression cycle. It is important to note that the term stiffness is often used to represent the Young's modulus of elasticity (E), which is a material property with units of newtons per square meter (or pascals). Here, the term stiffness refers simply to the resistance of the lens to compression (in millinewtons per millimeter). Resilience was measured from the same compression cycle by calculating the area under the unloading curve, dividing it by the area under the loading curve, and multiplying by 100%. Comparison of data from 0.06-, 0.12-, and 0.24-mm compression cycles revealed no differences in mechanical behavior or evidence of damage that appeared in subsequent cycles (i.e., force-compression curves were repeatable). Forces were highest in 0.24-mm cycles, which resulted in a higher signal-to-noise ratio for these data, compared with the smaller cycles. For this reason, the data presented here are from the final 0.24-mm cycle.

Statistical Analysis

Because we suspected that factors such as lens size, nuclear size, and age might have had significant effects on lens stiffness and resilience, we incorporated morphometric and age data into the statistical models used to evaluate the effect of genotype on these two mechanical properties. The models used were mixed general linear models that used type III sums of squares to evaluate the significance of covariate effects. Two lenses were tested from each mouse, and because stiffness and resilience values from lens pairs tended to resemble each other more than values from other mice (based on covariance parameter estimates), "mouse" was incorporated as a random effect in both models used. The final statistical models for both stiffness and resilience data were obtained by starting with a model that included all variables measured for every lens, which included lens volume, equatorial diameter, axial diameter, nuclear diameter, age, lens weight, and genotype. Because many of these variables are highly correlated, it was not necessary or desirable to include them all in the final models. The final models for stiffness and resilience were each determined by eliminating the variables with the highest P values one by one and rerunning the model. Only variables with low P values ($P < 0.10$) or variables that appeared in significant interaction terms were retained in the final model. This process resulted in the following variables in the final model for both the stiffness and resilience data: lens volume, genotype, age, and the genotype×age interactive effect. Effects of genotype and age on lens morphometrics were assessed with a general linear model (PASW Statistics ver. 17 software; SPSS, Chicago, IL).

RESULTS

Structural analysis of BF KO lenses revealed that the cells undergo a progressive, long-term loss of the differentiated phenotype with age. To ensure that these cells were alive, we compared specific physiological properties to the WT. The results of the impedance experiments are summarized in Table

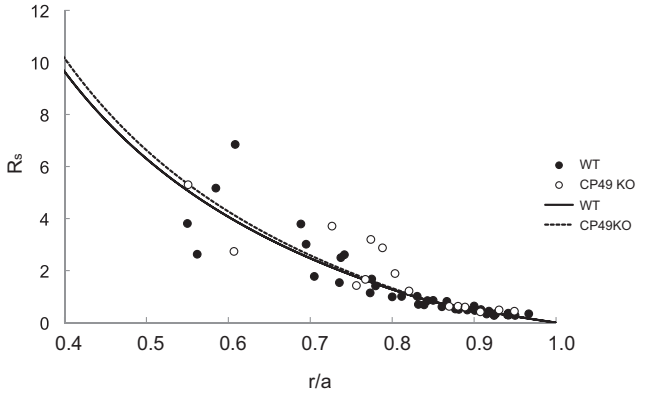

FIGURE 3. Series resistance data (R_S) from all lenses studied graphed as a function of distance from the lens center (r/a). The lens radius is a, and the location of the voltage recording electrode is r (both in centimeters) from the center. The best fit curves (*solid lines*) were generated from equations 2 and 3 and were used to determine G_{DF} and G_{MF} in Table 1.

1. There were no significant differences between WT and CP49 KO lenses with regard to any of the parameters measured. The input resistance and resting voltage are average values from 10 WT and 6 CP49 KO lenses. The values of gap-junction–coupling conductance in the outer shell of differentiating fibers (G_{DF}) and inner core of mature fibers (G_{MF}) were obtained by curve fitting equations 2 and 3 to the series resistance data from all lenses, as shown in Figure 3. Hence, these parameters do not have standard deviations, but one can see from Figure 3 how the data scatter around the best-fit curves (solid lines). The scatter increases with depth into the lenses, mostly because the location of the voltage recording electrode becomes increasingly difficult to determine accurately as the electrode is moved into the lens. CP49 is known to interact with lens gap junctions, so we were particularly interested in the effect of knocking out CP49 on coupling conductance. However, as can be seen in Table 1 and Figure 3, gap-junction–coupling conductance was not affected by the knockout.

Eye and Lens Morphometrics

Lens volume and weight increased linearly with age, with WT lenses being larger for a given age than CP49 KO lenses ($P < 0.01$; Fig. 4). Plots of lens axial diameter versus equatorial diameter were also linear and differed significantly ($P < 0.001$) between WT and CP49 KO lenses, with CP49 KO lenses having a higher ratio of D_{ax}:D_{eq} (Fig. 5). This result suggests that a lack of BFs has subtle effects on lens shape and size. Nuclear diameter increased with age and was greater at a given age in the WT lenses than in the CP49 KO lenses ($P < 0.01$; Fig. 6). To test whether the larger nuclear diameter in WT lenses was a consequence of the larger size of the WT lenses, we plotted nuclear diameter against lens volume and found that nuclear diameter was larger for a given lens volume in the WT than in the CP49 KO ($P < 0.001$; Fig. 6; Table 2). The relationship between lens weight and volume was linear, with WT lenses exhibiting an overall higher ratio of weight to volume (i.e., density; $P < 0.001$; Fig. 7), which is probably due to their possession of a greater nuclear volume.

Lens Stiffness

Lens volume had a strong positive effect on lens stiffness ($P = 0.014$), and therefore it was included in the final statistical model used to measure the effects of genotype. As predicted, CP49 KO lenses exhibited lower overall stiffness than did the WT lenses ($P = 0.004$; Figs. 8, 9), and this effect was most prominent in the young and middle-aged mice. Although age was not a significant determinant of stiffness ($P = 0.555$), it was kept in the model, because of a significant interactive effect between genotype and age ($P = 0.042$). This result means that complete knowledge of the genotype effects on stiffness requires knowing the age of the mice.

Lens Resilience

The effect of lens volume on resilience was not significant ($P = 0.10$), but it was kept in the final statistical model used to measure genotype effects, because it accounted for a considerable amount of the variation in the results. Genotype had a significant effect on resilience ($P = 0.0057$; Fig. 10), but not in the direction predicted, with young and old CP49 KO mice exhibiting greater resilience than their WT counterparts. Age was also a significant determinant of lens resilience ($P = 0.012$), as was the interaction between genotype and age ($P = 0.0096$). This result indicates that the effect of genotype on lens resilience depends on the age of the mice.

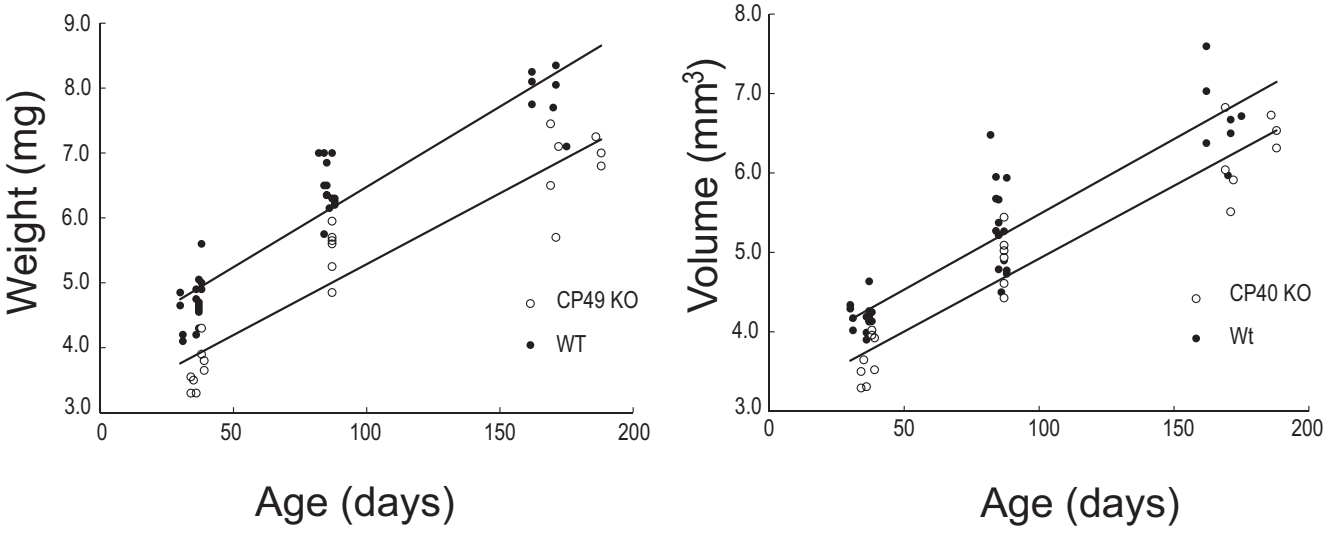

FIGURE 4. Changes in lens weight and volume with age. Beaded filament knockout results in significantly smaller ($P < 0.01$) lenses in all three age groups examined.

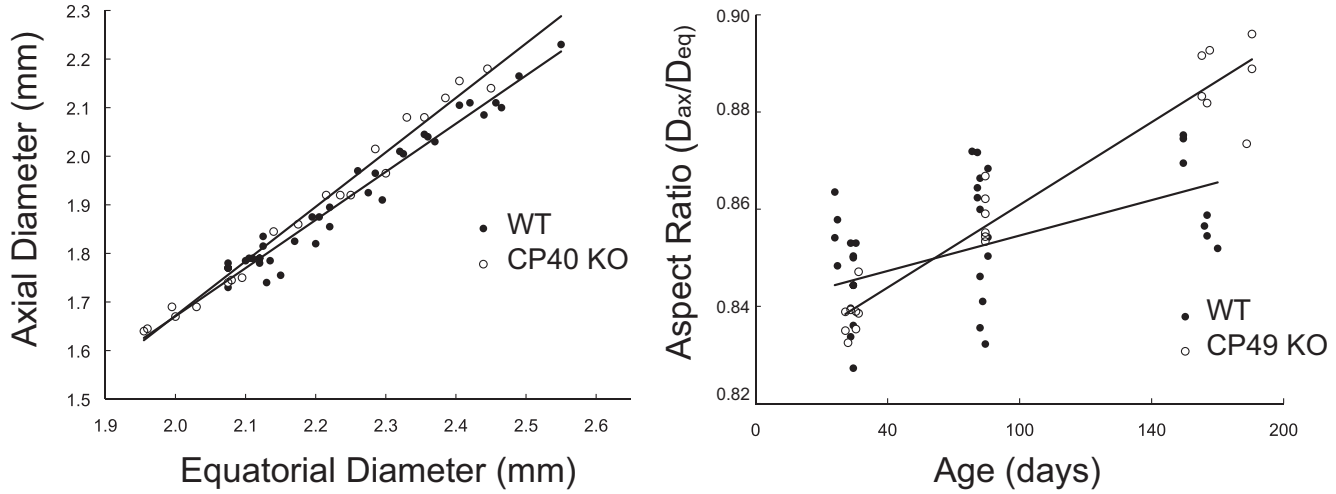

FIGURE 5. Relationship between lens axial and equatorial diameters (*left*) and lens aspect ratio (D_{ax}:D_{eq}) as a function of age (*right*). Note that that CP49 KO lenses have a significantly higher ($P < 0.001$) D_{ax}:D_{eq} ratio than WT lenses. These data suggest that BF knockout has subtle effects on lens shape in addition to size.

DISCUSSION

In this article, we present morphometric and biomechanical data for mouse lenses isolated from congenic strains differing only in the presence or absence of a lens-specific member of the IF family. These filaments are found only in the lens, and they are conserved among the vertebrates.[35] Based on work that has shown that IFs are necessary for the mechanical integrity of tissues such as skin and muscle,[24,27,36] we hypothesized that BFs in the lens are important for the structural integrity and mechanical properties of lens fiber cells and hence the entire lens. Although we found that BF knockout had no obvious effects on tissue integrity, our data clearly show that BFs make a significant contribution to the mechanical properties of the lens and have other unexpected effects on overall lens morphometrics.

Lens stiffness was higher in young and middle-aged WT mice than in their CP49 KO counterparts, but stiffnesses were similar between older WT and CP49 KO mice (Fig. 9). These results are consistent with those in other studies that have shown that IFs contribute to cell stiffness.[28] They also suggest that BFs are important in setting the mechanical properties of lenses in these younger mice and likely have direct implications for the function of the lenses in vivo. Specifically, the findings indicate that lenses lacking BFs require less force to be deformed a given amount. It also implies that CP49 KO animals possess a different relationship between the deforming force and optical power of the lens, which if not calibrated properly, could lead to difficulty with focusing. Such an effect would obviously be more important in species such as humans in which the magnitude of lens strain is believed to be larger than in the mouse. Because of the large size of the mouse lens and the very small size of the ciliary muscle, mice are generally not thought to be capable of any significant degree of accommodation, although, to the best of our knowledge this notion has not been directly proven.[37]

The fact that the genotype effect is absent in old mice suggests that lens stiffness is dominated by other age-dependent factors such as lens fiber cell compaction and/or dehydration. Other researchers who have measured lens mechanical properties have found significant age-related increases in

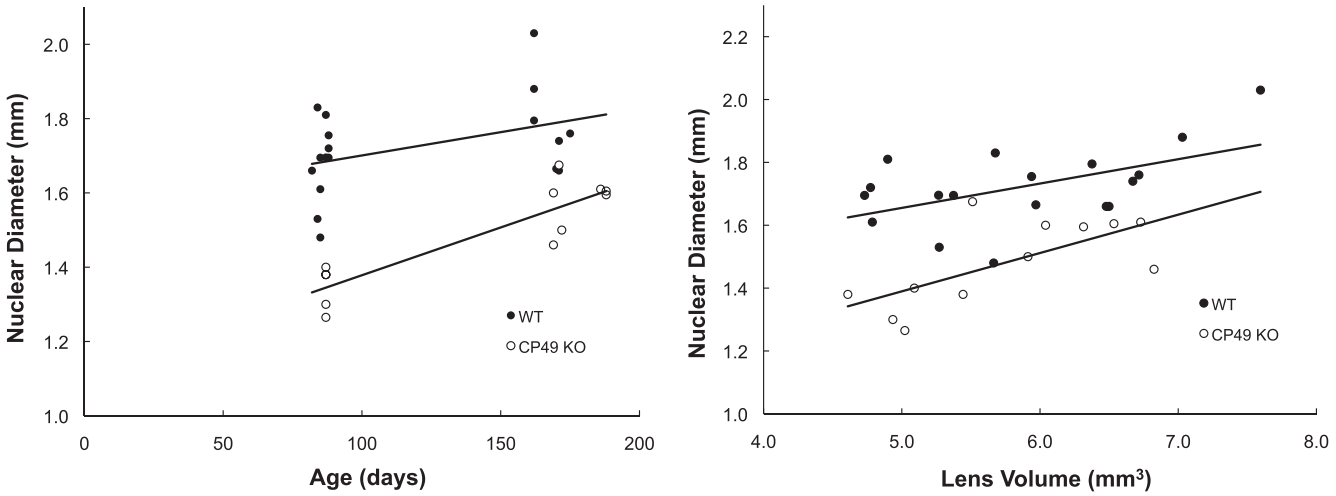

FIGURE 6. Nuclei were significantly larger in WT mice than in CP49 KO mice in both the middle-aged and old age groups ($P < 0.01$; nuclei were not visible in young mice). Regressions of nuclear diameter versus lens volume demonstrated that the differences in nuclear size between WT and CP49 KO mice are not simply a result of larger lens size in the WTs; nuclei are larger in WTs for a given lens volume as well ($P < 0.001$).

TABLE 2. Morphometrics of WT and CP49 KO Lenses

	D_{ax} (mm)	D_{eq} (mm)	Weight (mg)	Volume (mm^3)	D_{nuc} (mm)
WT, young	1.78 ± 0.03	2.12 ± 0.03	4.69 ± 0.38	4.18 ± 0.17	—
KO, young	1.70 ± 0.04	2.02 ± 0.05	3.66 ± 0.33	3.65 ± 0.29	—
WT, mid	1.95 ± 0.08	2.28 ± 0.07	6.46 ± 0.37	5.32 ± 0.57	1.65 ± 0.14
KO, mid	1.90 ± 0.04	2.22 ± 0.06	5.50 ± 0.39	4.92 ± 0.36	1.34 ± 0.06
WT, old	2.12 ± 0.06	2.45 ± 0.06	7.90 ± 0.43	6.69 ± 0.52	1.79 ± 0.13
KO, old	2.11 ± 0.06	2.38 ± 0.06	6.83 ± 0.58	6.27 ± 0.47	1.58 ± 0.07

Values are averages ± SD. D_{ax}, axial diameter; D_{eq}, equatorial diameter; D_{nuc}, nuclear diameter. Young lenses had no measurable nucleus. Genotype and age both had significant effects ($P < 0.01$) on all five parameters measured.

lens stiffness. In the human lens, nuclear stiffness increases by three orders of magnitude from the ages of 14 to 78 years.[38] A recent study of mouse lens mechanics found a significant increase in lens stiffness with age.[39] The larger age effect found by these researchers in the mouse lens was probably due to their use of a larger age range than in the present study, with their oldest mice being 36 weeks old.

We also hypothesized that BFs contribute to the ability of lenses to elastically recover from deformations, but surprisingly found evidence to the contrary. Specifically, we found that resilience was higher in CP49 KO mice than in WT mice in both the young and old age groups. These results suggest that the absence of BF in lens fiber cells imparts greater elasticity to the lens, although the effect is modest, and they mean that a greater proportion of the strain energy that goes into the lens during compression is returned as the compressor returns to its starting point of 0 strain. Another way of thinking about this phenomenon is that a higher proportion of strain energy was lost in the WT than in the CP49 KO lenses, although it is not clear whether this energy was dissipated as heat or was consumed during processes that irreversibly damaged the lens. A possible explanation for the effect is that BFs act simply to increase the viscosity of the cytoplasm in fiber cells. For this hypothesis to be viable, lens deformation would have to involve cytoplasmic flow within fiber cells, which is an intriguing possibility that we intend to explore in future studies. If the primary mechanical function of BFs is to increase the viscosity of fiber cell cytoplasm, it would be consistent with our finding that BFs appear to have no influence on tissue integrity.

The relative contribution of fiber cells to the overall elasticity of the lens remains controversial. Helmholtz was the first to propose that the lens is flattened via the action of zonular ligaments and returns to a more rounded state via elastic recoil. He did not, however, specify whether lens elasticity arises from the collagenous capsule or the lens substance (consisting of the fiber cells). Fincham[40] proposed that lenticular elasticity is almost exclusively due to the capsule, which simply molds a viscous lens substance. Weale[41] and Fisher[42,43] suggested that the lens substance is not a purely viscous material, but possesses some inherent elasticity that contributes to elastic recoil. More recent studies have demonstrated that the capsule and the lens substance are both viscoelastic,[44–47] and the capsule acts to evenly distribute forces from the attached zonule fibers.[48] Our data suggest that changes in the fiber cells that make up the lens substance can have significant effects on overall lens morphometrics and mechanical behavior.

Besides causing significant effects on lens mechanics, CP49 KO also had surprising effects on lens morphometrics. Most important, CP49 KO lenses were smaller for a given age and possessed smaller nuclei for a given age and for a given lens volume. These results are consistent with a finding by Zhou and Williams[49] that showed a smaller lens size in 129/SvJ mice than in C57BL/6J mice, despite a nearly identical eye size. This is relevant to our data, because the 129/SvJ strain is known to be a functional BF knockout due to a mutation in the CP49 gene.[10,21] Although the mechanisms by which BF regulate lens and nuclear growth are not clear, we find it interesting that targeted deletion of a single gene can have predictable effects on the size and organization of a single tissue. One question that comes out of the morphometrics results is whether the smaller lenses in KO mice arise from slower rates of cell proliferation in the lens epithelium, smaller fiber cells, or a

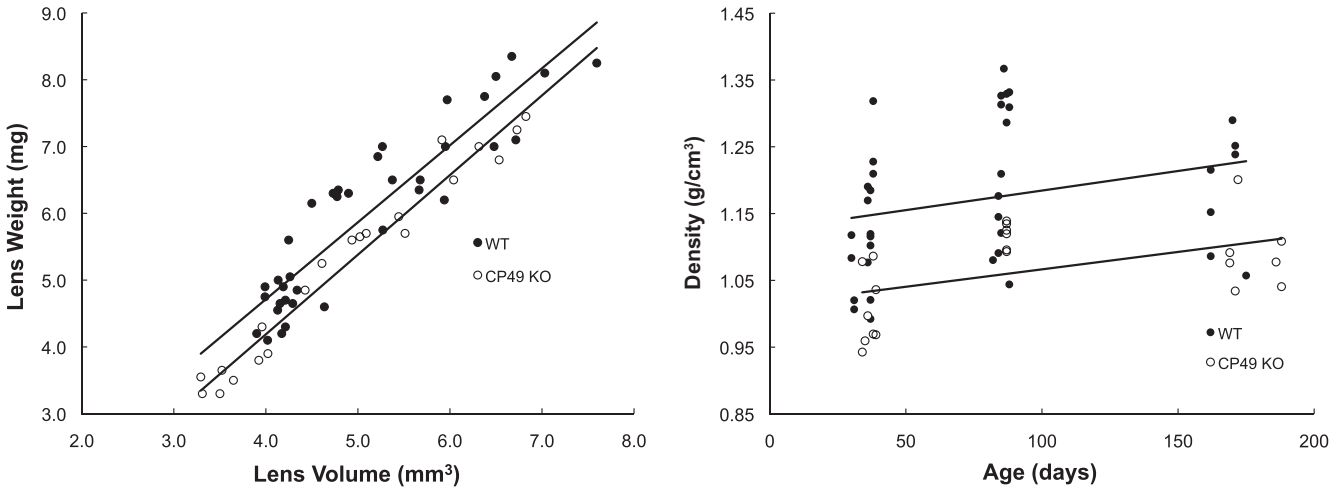

FIGURE 7. Lens weight plotted against volume (*left*) and density, as a function of age (*right*). WT lenses were significantly heavier ($P < 0.001$) for a given lens volume. The higher density of WT lenses is most likely a consequence of their possessing larger nuclei.

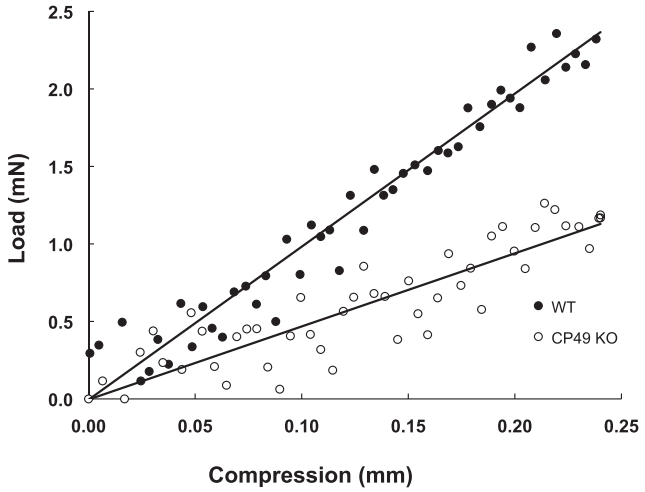

FIGURE 8. Typical data used for the measurement of lens stiffness. Load was measured as lenses were compressed with a custom compression device to an extension of 0.24 mm. Stiffnesses were calculated as the slope of the load-compression curves. Although the data are noisy because of the small forces generated by the lenses, repeatable, and significant differences in stiffness were measured between the WT and CP49 KO lenses.

combination of the two. Other researchers have found that IF knockout can lead to smaller cell size in mice, with keratin 8 knockout leading to smaller hepatocytes[50] and keratin 17 knockout leading to smaller keratinocytes.[51] We attempted to explore this issue by examining SEM images of fixed WT and KO lenses (data not shown), but the irregular shape and packing of fiber cells in KO lenses prevented the accurate estimation of cell dimensions that is possible in uniform, regularly packed WT fiber cells.

Although we have clearly shown that CP49 KO has consequences for the size and mechanical behavior of murine lenses, future work should attempt to characterize the implications of these changes on the function of lenses in vivo. Specifically, mechanical testing coupled with finite element modeling would provide a clearer picture of how the material properties of the lens substance are altered. Similarly, deforming the lenses in a way that mimics the action of the zonular fibers while measuring optical power would provide further insights into the functional contributions that BF make to the ocular lens.

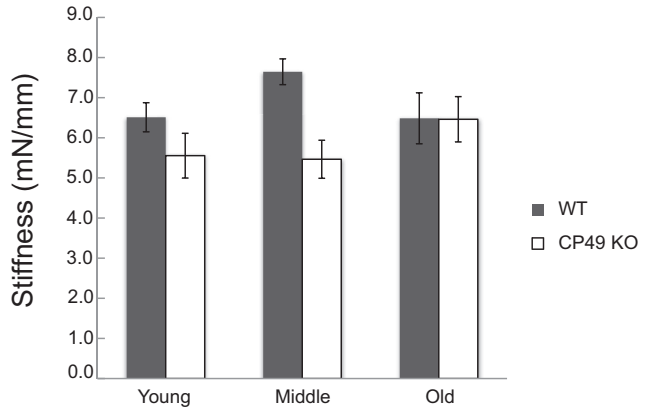

FIGURE 9. Mean stiffnesses (±SE) in young, middle-aged, and old mice. Stiffness values were measured as the slope of load-compression curves and were found to be significantly higher in WT lenses ($P < 0.01$).

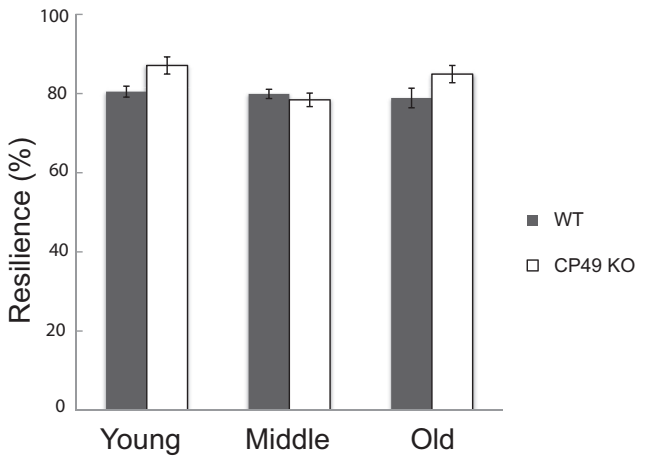

FIGURE 10. Average resilience values (±SE) for young, middle-aged, and old mice. Resilience is defined as the percentage of strain energy recovered during unloading of the lenses. Strain energy was calculated as the area under the loading curve, and recovered energy was calculated as the area under the unloading curve. Lenses from CP49 KO mice were significantly more resilient than were the WT lenses ($P < 0.01$).

Acknowledgments

The authors thank Steve Wilson for the construction of the lens compression chamber, the staff at the Central Animal Facility at the University of Guelph, and Sanjeena Subedi and Brian Allen at the Ashton Statistical Laboratory.

References

1. Fawcett D. Textbook of Histology. 1994;892.
2. Helmholtz H. 1. Uber die Akkommodation des Auges. *Albrecht von Graefes Arch Klin Ophthalmol.* 1855;1:1–74.
3. Kuwabara T. The maturation of the lens cell: a morphologic study. *Exp Eye Res.* 1975;20:427–443.
4. Wanko T, Gavin MA. Electron microscope study of lens fibers. *J Biophys Biochem Cytol.* 1959;6:97–102.
5. Cohen AI. Electron microscopic observations on the lens of the neonatal albino mouse. *Am J Anat.* 1958;103:219–245.
6. Kuszak JR, Macsai MS, Rae JL. Stereo scanning electron microscopy of the crystalline lens. *Scan Electron Microsc.* 1983;1415–1426.
7. Kuszak JR, Peterson KL, Brown HG. Electron microscopic observations of the crystalline lens. *Microsc Res Tech.* 1996;33:441–479.
8. Kuszak JR, Rae JL. Scanning electron microscopy of the frog lens. *Exp Eye Res.* 1982;35:499–519.
9. Yoon KH, Blankenship T, Shibata B, Fitzgerald PG. Resisting the effects of aging: a function for the fiber cell beaded filament. *Invest Ophthalmol Vis Sci.* 2008;49:1030–1036.
10. Sandilands A, Prescott AR, Wegener A, et al. Knockout of the intermediate filament protein CP49 destabilises the lens fibre cell cytoskeleton and decreases lens optical quality, but does not induce cataract. *Exp Eye Res.* 2003;76:385–391.
11. Kuwabara T, Imaizumi M. Denucleation process of the lens. *Invest Ophthalmol.* 1974;13:973–981.
12. Bassnett S. Mitochondrial dynamics in differentiating fiber cells of the mammalian lens. *Curr Eye Res.* 1992;11:1227–1232.
13. Bassnett S, Beebe DC. Coincident loss of mitochondria and nuclei during lens fiber cell differentiation. *Dev Dyn.* 1992;194:85–93.
14. Lovicu F, Robinson M, eds. *Development of the Ocular Lens*. New York: Cambridge University Press; 2004.
15. Ireland M, Maisel H. A cytoskeletal protein unique to lens fiber cell differentiation. *Exp Eye Res.* 1984;38:637–645.
16. Ireland M, Maisel H. A family of lens fiber cell specific proteins. *Lens Eye Toxic Res.* 1989;6:623–638.
17. FitzGerald PG. Immunochemical characterization of a Mr 115 lens fiber cell-specific extrinsic membrane protein. *Curr Eye Res.* 1988; 7:1243–1253.

18. Maisel H. Filaments of the vertebrate lens. *Experientia.* 1977;33:525.
19. Maisel H, Perry MM. Electron microscope observations on some structural proteins of the chick lens. *Exp Eye Res.* 1972;14:7–12.
20. Alizadeh A, Clark J, Seeberger T, Hess J, Blankenship T, FitzGerald PG. Targeted deletion of the lens fiber cell-specific intermediate filament protein filensin. *Invest Ophthalmol Vis Sci.* 2003;44:5252–5258.
21. Alizadeh A, Clark JI, Seeberger T, et al. Targeted genomic deletion of the lens-specific intermediate filament protein CP49. *Invest Ophthalmol Vis Sci.* 2002;43:3722–3727.
22. Conley YP, Erturk D, Keverline A, et al. A juvenile-onset, progressive cataract locus on chromosome 3q21–q22 is associated with a missense mutation in the beaded filament structural protein-2. *Am J Hum Genet.* 2000;66:1426–1431.
23. Jakobs PM, Hess JF, FitzGerald PG, Kramer P, Weleber RG, Litt M. Autosomal-dominant congenital cataract associated with a deletion mutation in the human beaded filament protein gene BFSP2. *Am J Hum Genet.* 2000;66:1432–1436.
24. Coulombe PA, Hutton ME, Vassar R, Fuchs E. A function for keratins and a common thread among different types of epidermolysis bullosa simplex diseases. *J Cell Biol.* 1991;115:1661–1674.
25. Ishida-Yamamoto A, McGrath JA, Chapman SJ, Leigh IM, Lane EB, Eady RA. Epidermolysis bullosa simplex (Dowling-Meara type) is a genetic disease characterized by an abnormal keratin-filament network involving keratins K5 and K14. *J Invest Dermatol.* 1991;97:959–968.
26. Capetanaki Y, Milner DJ. Desmin cytoskeleton in muscle integrity and function. *Subcell Biochem.* 1998;31:463–495.
27. Capetanaki Y, Milner DJ, Weitzer G. Desmin in muscle formation and maintenance: knockouts and consequences. *Cell Struct Funct.* 1997;22:103–116.
28. Wang N, Stamenovic D. Contribution of intermediate filaments to cell stiffness, stiffening, and growth. *Am J Physiol Cell Physiol.* 2000;279:C188–C194.
29. Bertaud J, Qin Z, Buehler MJ. Intermediate filament-deficient cells are mechanically softer at large deformation: a multi-scale simulation study. *Acta Biomater.* 2010;6:2457–2466.
30. Fudge D, Russell D, Beriault D, Moore W, Lane EB, Vogl AW. The intermediate filament network in cultured human keratinocytes is remarkably extensible and resilient. *PLoS One.* 2008;3:e2327.
31. Fudge DS, Gosline JM. Molecular design of the alpha-keratin composite: insights from a matrix-free model, hagfish slime threads. *Proc Biol Sci.* 2004;271:291–299.
32. Alizadeh A, Clark J, Seeberger T, Hess J, Blankenship T, FitzGerald PG. Characterization of a mutation in the lens-specific CP49 in the 129 strain of mouse. *Invest Ophthalmol Vis Sci.* 2004;45:884–891.
33. Simirskii VN, Lee RS, Wawrousek EF, Duncan MK. Inbred FVB/N mice are mutant at the cp49/Bfsp2 locus and lack beaded filament proteins in the lens. *Invest Ophthalmol Vis Sci.* 2006;47:4931–4934.
34. Wang H, Gao J, Sun X, et al. The effects of GPX-1 knockout on membrane transport and intracellular homeostasis in the lens. *J Membr Biol.* 2009;227:25–37.
35. FitzGerald PG, Casselman J. Immunologic conservation of the fiber cell beaded filament. *Curr Eye Res.* 1991;10:471–478.
36. Capetanaki Y, Milner DJ. Desmin cytoskeleton in muscle integrity and function. In: Herrmann H, Harris JR eds. *Intermediate Filaments*. New York: Plenum Press; 1998;463–495.
37. Smith RM, Sundberg JP, John SWM. The anterior segment and ocular adnexa. In: Smith RS, ed. *Systematic Evaluation of the Mouse Eye*: *Anatomy*, *Pathology*, *and Biomethods*. New York: CRC Press; 2002;3–24.
38. Heys KR, Cram SL, Truscott RJ. Massive increase in the stiffness of the human lens nucleus with age: the basis for presbyopia? *Mol Vis.* 2004;10:956–963.
39. Baradia H, Nikahd N, Glasser A. Mouse lens stiffness measurements. *Exp Eye Res.* 2010;91:300–307.
40. Fincham E. The mechanism of accommodation. *Br J Ophthalmol.* 1937;21:5–80.
41. Weale RA. Presbyopia. *Br J Ophthalmol.* 1962;46:660–668.
42. Fisher RF. Elastic constants of the human lens capsule. *J Physiol.* 1969;201:1–19.
43. Fisher RF. The significance of the shape of the lens and capsular energy changes in accommodation. *J Physiol.* 1969;201:21–47.
44. Beers AP, van der Heijde GL. Age-related changes in the accommodation mechanism. *Optom Vis Sci.* 1996;73:235–242.
45. Krag S, Olsen T, Andreassen TT. Biomechanical characteristics of the human anterior lens capsule in relation to age. *Invest Ophthalmol Vis Sci.* 1997;38:357–363.
46. Glasser A, Campbell MC. Biometric, optical and physical changes in the isolated human crystalline lens with age in relation to presbyopia. *Vision Res.* 1999;39:1991–2015.
47. Tiffany JM, Koretz JF. Viscosity of alpha-crystallin solutions. *Int J Biol Macromol.* 2002;30:179–185.
48. Koretz JF, Handelman GH. Model of the accommodative mechanism in the human eye. *Vision Res.* 1982;22:917–927.
49. Zhou G, Williams RW. Eye1 and eye2: gene loci that modulate eye size, lens weight, and retinal area in the mouse. *Invest Ophthalmol Vis Sci.* 1999;40:817–825.
50. Galarneau L, Loranger A, Gilbert S, Marceau N. Keratins modulate hepatic cell adhesion, size and G1/S transition. *Exp Cell Res.* 2007;313:179–194.
51. Kim S, Wong P, Coulombe PA. A keratin cytoskeletal protein regulates protein synthesis and epithelial cell growth. *Nature.* 2006;441:362–365.